

## The invariant Rauch-Tung-Striebel Smoother

N. van der Laan,  
J. Arsenault, J. R. Forbes

G-2019-99

December 2019

---

La collection *Les Cahiers du GERAD* est constituée des travaux de recherche menés par nos membres. La plupart de ces documents de travail a été soumis à des revues avec comité de révision. Lorsqu'un document est accepté et publié, le pdf original est retiré si c'est nécessaire et un lien vers l'article publié est ajouté.

**Citation suggérée :** N. van der Laan, J. Arsenault, J. R. Forbes (Décembre 2019). The invariant Rauch-Tung-Striebel Smoother, Rapport technique, Les Cahiers du GERAD G-2019-99, GERAD, HEC Montréal, Canada.

**Avant de citer ce rapport technique**, veuillez visiter notre site Web (<https://www.gerad.ca/fr/papers/G-2019-99>) afin de mettre à jour vos données de référence, s'il a été publié dans une revue scientifique.

---

La publication de ces rapports de recherche est rendue possible grâce au soutien de HEC Montréal, Polytechnique Montréal, Université McGill, Université du Québec à Montréal, ainsi que du Fonds de recherche du Québec – Nature et technologies.

Dépôt légal – Bibliothèque et Archives nationales du Québec, 2019  
– Bibliothèque et Archives Canada, 2019

The series *Les Cahiers du GERAD* consists of working papers carried out by our members. Most of these pre-prints have been submitted to peer-reviewed journals. When accepted and published, if necessary, the original pdf is removed and a link to the published article is added.

**Suggested citation:** N. van der Laan, J. Arsenault, J. R. Forbes (December 2019). The invariant Rauch-Tung-Striebel Smoother, Technical report, Les Cahiers du GERAD G-2019-99, GERAD, HEC Montréal, Canada.

**Before citing this technical report**, please visit our website (<https://www.gerad.ca/en/papers/G-2019-99>) to update your reference data, if it has been published in a scientific journal.

---

The publication of these research reports is made possible thanks to the support of HEC Montréal, Polytechnique Montréal, McGill University, Université du Québec à Montréal, as well as the Fonds de recherche du Québec – Nature et technologies.

Legal deposit – Bibliothèque et Archives nationales du Québec, 2019  
– Library and Archives Canada, 2019



# The invariant Rauch-Tung-Striebel Smoother

Niels van der Laan<sup>a</sup>

Jonathan Arsenault<sup>b</sup>

James Richard Forbes<sup>a,b</sup>

<sup>a</sup> GERAD, Montréal (Québec), Canada, H3T 2A7

<sup>b</sup> Department of Mechanical Engineering, McGill University, Montréal (Québec) Canada, H3A 0C3

niels.vanderlaan@mail.mcgill.ca

jonathan.arsenault@mail.mcgill.ca

james.richard.forbes@mcgill.ca

December 2019

Les Cahiers du GERAD  
G–2019–99

Copyright © 2019 GERAD, van der Laan, Arsenault, Forbes, IEEE. This paper is a preprint (IEEE “submitted” status). Personal use of this material is permitted. Permission from IEEE must be obtained for all other uses, in any current or future media, including reprinting/republishing this material for advertising or promotional purposes, creating new collective works, for resale or redistribution to servers or lists, or reuse of any copyrighted component of this work in other works.

---

Les textes publiés dans la série des rapports de recherche *Les Cahiers du GERAD* n’engagent que la responsabilité de leurs auteurs. Les auteurs conservent leur droit d’auteur et leurs droits moraux sur leurs publications et les utilisateurs s’engagent à reconnaître et respecter les exigences légales associées à ces droits. Ainsi, les utilisateurs:

- Peuvent télécharger et imprimer une copie de toute publication du portail public aux fins d’étude ou de recherche privée;
- Ne peuvent pas distribuer le matériel ou l’utiliser pour une activité à but lucratif ou pour un gain commercial;
- Peuvent distribuer gratuitement l’URL identifiant la publication.

Si vous pensez que ce document enfreint le droit d’auteur, contactez-nous en fournissant des détails. Nous supprimerons immédiatement l’accès au travail et enquêterons sur votre demande.

The authors are exclusively responsible for the content of their research papers published in the series *Les Cahiers du GERAD*. Copyright and moral rights for the publications are retained by the authors and the users must commit themselves to recognize and abide the legal requirements associated with these rights. Thus, users:

- May download and print one copy of any publication from the public portal for the purpose of private study or research;
- May not further distribute the material or use it for any profit-making activity or commercial gain;
- May freely distribute the URL identifying the publication.

If you believe that this document breaches copyright please contact us providing details, and we will remove access to the work immediately and investigate your claim.

**Abstract:** This paper presents an invariant Rauch-Tung-Striebel Smoother (IRTS) applicable to systems with states that are an element of a matrix Lie group. In particular, the extended Rauch-Tung-Striebel (RTS) smoother is adapted to work within a matrix Lie group framework. The main advantage of the invariant RTS (IRTS) smoother is that the linearization of the process and measurement models is independent of the state estimate resulting in state independent Jacobians when certain technical requirements are met. The multiplicative RTS (MRTS) smoother is also reviewed and is used as a direct comparison to the proposed IRTS smoother using simulated and experimental data.

---

**Acknowledgments:** The authors graciously acknowledge funding from Group for Research in Decision Analysis (GERAD) and the National Science and Engineering Research Council (NSERC) of Canada.

# 1 Introduction

The need to estimate states using incomplete and noisy data arises in many engineering applications. In robotics applications, where states of interest are often elements of a matrix Lie group, a popular state estimator is the extended Kalman filter (EKF), or rather the multiplicative extended Kalman filter (MEKF), a variant of the EKF [1]. The EKF is an approximation to the Bayes filter that uses linearization to compute a state estimate [2, Sec. 4.2]. The prediction and correction steps of the EKF use process and measurement model Jacobians, respectively, that are evaluated at the most recent state estimate. If the most recent state estimate is poor, the Jacobians are inaccurate.

The invariant EKF (IEKF) is a state estimator that is specific to systems with states that are an element of a matrix Lie group. It was shown in [3, 4] that when the process model is group affine, the measurements are left invariant (right invariant), and a left-invariant error (right-invariant error) is used, the IEKF as interpreted as an observer possesses asymptotic convergence properties. Moreover, the Jacobians associated with the IEKF are state-estimate independent and, as such, the IEKF has enhanced performance properties when compared to the EKF or MEKF [3, 4].

Unlike the Kalman filter and its nonlinear variants, the Rauch-Tung-Striebel (RTS) smoother uses all available measurements in a batch framework to compute state estimates using a forward pass followed by a backward pass. In [5] an RTS smoother for systems with states that are an element of a matrix Lie group is presented, but the invariant framework is not leveraged. The article [6] considers the full batch estimation problem in an invariant framework, rather than a forward-backward smoothing approach, as considered in [5] and this paper. The advantage of the IEKF framework is the fact that the Jacobians are state-estimate independent. Motivated by this fact, this paper considers the derivation of an invariant RTS (IRTS) smoother for systems with states that are elements of a matrix Lie group. Like the IEKF, the IRTS smoother has state-independent Jacobians.

To assess the performance of the IRTS smoother relative to a multiplicative RTS (MRTS) smoother, a state estimation problem on the matrix Lie group  $SE_2(3)$  is considered. In particular, the position, attitude and velocity of a rigid body are estimated using accelerometer, rate gyro, and position measurements. Simulation results demonstrate that the state-estimate independent Jacobians associated with the IRTS smoother result in better performance relative to the MRTS smoother that uses state-estimate-dependent Jacobians. Experimental results using the EuRoC dataset [7] is also considered. Although results are less pronounced when working with real data, the IRTS smoother outperforms the MRTS smoother.

The remainder of this paper is as follows. Notation and preliminaries are presented in Section 2. In Section 3 the standard RTS smoother is reviewed. An extended RTS smoother applicable to systems with states that are an element of matrix Lie group, a so-called MRTS smoother, is presented in Section 4. Finally, the IEKF framework is brought to bear on the RTS smoothing problem in Section 5. Section 6 formulates the state estimation problem associated with  $SE_2(3)$ , while Sections 7.1 and 7.2 present simulation and experimental results of the MRTS and IRTS smoothers applied to the  $SE_2(3)$  estimation problem. The paper is drawn to a close in Section 8. This paper's contributions are the IRTS smoother derivation in Section 5 and its evaluation in simulation and experiments in Sections 7.1 and 7.2.

## 2 Preliminaries

### 2.1 Matrix Lie groups

Consider the matrix Lie group  $\mathcal{G}$ , which is composed of  $n \times n$  matrices with  $m$  degrees of freedom, that is closed under matrix multiplication [8]. The matrix Lie algebra associated with  $\mathcal{G}$ , denoted by  $\mathfrak{g}$ , is the tangent space of  $\mathcal{G}$  at the identity element  $\mathbf{1}$ , denoted as  $T_1\mathcal{G}$ . The matrix Lie algebra can be mapped to the matrix Lie group using the exponential map,  $\exp(\cdot) : \mathfrak{g} \rightarrow \mathcal{G}$ . The inverse map uses

the matrix natural logarithm,  $\ln(\cdot) : \mathcal{G} \rightarrow \mathfrak{g}$ . The linear operator  $(\cdot)^\wedge : \mathbb{R}^m \rightarrow \mathfrak{g}$  maps an  $m$  dimension column matrix to the matrix Lie algebra. The inverse map is  $(\cdot)^\vee : \mathfrak{g} \rightarrow \mathbb{R}^m$ .

*Definition 1 (Group Affine [3]):* The function  $\mathbf{F}(\mathbf{X}, \mathbf{u})$  is said to be group affine if for  $\mathbf{X}_1, \mathbf{X}_2 \in \mathcal{G}$  it satisfies

$$\mathbf{F}(\mathbf{X}_1 \mathbf{X}_2, \mathbf{u}) = \mathbf{X}_1 \mathbf{F}(\mathbf{X}_2, \mathbf{u}) + \mathbf{F}(\mathbf{X}_1, \mathbf{u}) \mathbf{X}_2 - \mathbf{X}_1 \mathbf{F}(\mathbf{1}, \mathbf{u}) \mathbf{X}_2.$$

*Definition 2 (Left- and Right-Invariant Error [3]):* Consider  $\mathbf{X}, \hat{\mathbf{X}} \in \mathcal{G}$ . The left-invariant error between  $\mathbf{X}$  and  $\hat{\mathbf{X}}$  is given by  $\delta \mathbf{X}^L = \mathbf{X}^{-1} \hat{\mathbf{X}}$  and the right-invariant error between  $\mathbf{X}$  and  $\hat{\mathbf{X}}$  is  $\delta \mathbf{X}^R = \hat{\mathbf{X}} \mathbf{X}^{-1}$ .

## 2.2 Kinematics

A reference frame  $\mathcal{F}_a$  is composed of three orthonormal physical basis vectors [9]. The orientation of  $\mathcal{F}_a$  relative to  $\mathcal{F}_b$  is described by a direction cosine matrix (DCM)  $\mathbf{C}_{ab} \in SO(3)$ . A physical vector  $\underline{y}$  can be resolved in  $\mathcal{F}_a$  as a column matrix  $\mathbf{v}_a$  or in  $\mathcal{F}_b$  as  $\mathbf{v}_b$ , where  $\mathbf{v}_a = \mathbf{C}_{ab} \mathbf{v}_b$  and  $\mathbf{v}_a, \mathbf{v}_b \in \mathbb{R}^3$ . The position of a point  $z$  relative to a point  $w$  resolved in  $\mathcal{F}_a$  is denoted as  $\mathbf{r}_a^{zw} \in \mathbb{R}^3$ . The velocity of  $z$  relative to  $w$  with respect to  $\mathcal{F}_a$  is denoted as  $\dot{\mathbf{r}}_a^{zw} = \mathbf{v}_a^{zw/a}$  and the angular velocity of  $\mathcal{F}_b$  relative to  $\mathcal{F}_a$  resolved in  $\mathcal{F}_c$  is given by  $\boldsymbol{\omega}_c^{ba} \in \mathbb{R}^3$ .

## 3 RTS smoothing

Consider the linear system

$$\dot{\mathbf{x}}(t) = \mathbf{A}\mathbf{x}(t) + \mathbf{B}\mathbf{u}(t) + \mathbf{L}\mathbf{w}(t), \quad (1)$$

$$\mathbf{y}_k = \mathbf{H}_k \mathbf{x}_k + \mathbf{M}_k \mathbf{v}_k, \quad (2)$$

where  $k$  denotes the time steps such that  $\mathbf{x}_k = \mathbf{x}(t_k)$ ,  $\mathbf{x}(t) \in \mathbb{R}^m$  is the state,  $\mathbf{u}(t)$  is an interoceptive measurement,  $\mathbf{y}_k$  is the exteroceptive measurement,  $\mathbf{w}(t)$  is process noise, and  $\mathbf{v}_k$  is measurement noise. Unless required for clarity, the argument  $(t)$  will once again be omitted for brevity. The discrete-time process model can be found in several ways [10] resulting in the discrete-time process model

$$\mathbf{x}_k = \mathbf{A}_{k-1} \mathbf{x}_{k-1} + \mathbf{B}_{k-1} \mathbf{u}_{k-1} + \mathbf{L}_{k-1} \mathbf{w}_{k-1}. \quad (3)$$

The RTS smoother consists of a forward filter and a smoother that goes backward in time. The forward filter is the traditional Kalman filter for  $k = 0, \dots, N$ .

The predicted state estimate and covariance are found using [11, Sec. 8.2]

$$\check{\mathbf{x}}_{fk} = \mathbf{A}_{k-1} \hat{\mathbf{x}}_{f,k-1} + \mathbf{B}_{k-1} \mathbf{u}_{k-1}, \quad (4)$$

$$\check{\mathbf{P}}_{fk} = \mathbf{A}_{k-1} \hat{\mathbf{P}}_{f,k-1} \mathbf{A}_{k-1}^\top + \mathbf{L}_{k-1} \mathbf{Q}_{k-1} \mathbf{L}_{k-1}^\top, \quad (5)$$

where  $\mathbf{w}_k \sim \mathcal{N}(\mathbf{0}, \mathbf{Q}_k)$ ,  $\check{\mathbf{x}}_{fk}$  is the *a priori* forward state estimate,  $\hat{\mathbf{x}}_{fk}$  is the *a posteriori* forward state estimate,  $\check{\mathbf{P}}_{fk}$  is the *a priori* forward covariance estimate and  $\hat{\mathbf{P}}_{fk}$  is the *a posteriori* forward covariance estimate. The Kalman gain  $\mathbf{K}_k$  is found by minimizing the covariance with respect to  $\mathbf{K}_k$ , which gives [11, Sec. 8.2]

$$\mathbf{K}_{fk} = \check{\mathbf{P}}_{fk} \mathbf{H}_k^\top (\mathbf{H}_k \check{\mathbf{P}}_{fk} \mathbf{H}_k^\top + \mathbf{M}_{k-1} \mathbf{R}_k \mathbf{M}_{k-1}^\top)^{-1}, \quad (6)$$

where  $\mathbf{v}_k \sim \mathcal{N}(\mathbf{0}, \mathbf{R}_k)$ . The predicted estimates are then updated using [12, Sec. 9.4]

$$\hat{\mathbf{x}}_{fk} = \check{\mathbf{x}}_{fk} + \mathbf{K}_{fk} (\mathbf{y}_k - \mathbf{H}_k \check{\mathbf{x}}_{fk}), \quad (7)$$

$$\begin{aligned} \hat{\mathbf{P}}_{fk} &= (\mathbf{1} - \mathbf{K}_{fk} \mathbf{H}_k) \check{\mathbf{P}}_{fk} (\mathbf{1} - \mathbf{K}_{fk} \mathbf{H}_k)^\top \\ &\quad + \mathbf{K}_{fk} \mathbf{M}_k \mathbf{R}_k \mathbf{M}_k^\top \mathbf{K}_{fk}^\top. \end{aligned} \quad (8)$$

After the forward filter has been run, the backward smoother is initialized using  $\hat{\mathbf{x}}_{fN}$  and  $\hat{\mathbf{P}}_{fN}$ . The smoothing equations [11, Sec. 8.2]

$$\mathbf{K}_{sk} = \hat{\mathbf{P}}_{fk} \mathbf{A}_k^T \check{\mathbf{P}}_{f,k+1}^{-1}, \quad (9)$$

$$\hat{\mathbf{x}}_{sk} = \hat{\mathbf{x}}_{fk} + \mathbf{K}_{sk} (\hat{\mathbf{x}}_{s,k+1} - \check{\mathbf{x}}_{f,k+1}), \quad (10)$$

$$\hat{\mathbf{P}}_{sk} = \hat{\mathbf{P}}_{fk} - \mathbf{K}_{sk} (\check{\mathbf{P}}_{f,k+1} - \hat{\mathbf{P}}_{s,k+1}) \mathbf{K}_{sk}^T, \quad (11)$$

are then used for  $k = N - 1, \dots, 0$ , where  $\mathbf{K}_{sk}$  is the smoother gain,  $\hat{\mathbf{x}}_{sk}$  is the smoother estimate, and  $\hat{\mathbf{P}}_{sk}$  is the smoother covariance.

## 4 Multiplicative RTS smoothing

The extended RTS smoother is used for nonlinear systems and has many variations, an example of which is discussed by Särkkä in [11]. Consider a nonlinear system described by the continuous-time process and discrete-time measurement models

$$\dot{\mathbf{X}}(t) = \mathbf{F}(\mathbf{X}(t), \mathbf{x}(t), \mathbf{u}(t), \mathbf{w}(t)), \quad (12)$$

$$\dot{\mathbf{x}}(t) = \mathbf{f}(\mathbf{X}(t), \mathbf{x}(t), \mathbf{u}(t), \mathbf{w}(t)), \quad (13)$$

$$\mathbf{y}_k = \mathbf{g}_k(\mathbf{x}_k, \mathbf{v}_k), \quad (14)$$

where  $\mathbf{X} \in \mathcal{G}$  is an element of a matrix Lie group while  $\mathbf{x} \in \mathbb{R}^{n_x}$ . For a process model of the form given by (12) and (13), the multiplicative RTS (MRTS) smoother can be used for state estimation. A similar multiplicative approach to smoothing is taken in [13, 5]. The MRTS smoother can be viewed as an extension of the extended RTS smoother in the same way the multiplicative extended Kalman Filter (MEKF) is an extension of the standard EKF. Owing to the popularity of the EKF, and the use of the MEKF as the benchmark when assessing the benefits of the IEKF, the MRTS smoother will be compared to the proposed IRTS smoother derived in Section 5.

As is done in many Kalman filter variants, the MRTS smoother requires linearization of the process and measurement models. Combining and linearizing (12) and (13), and also linearizing (14), results in

$$\delta \dot{\mathbf{x}} = \mathbf{A} \delta \mathbf{x} + \mathbf{L} \delta \mathbf{w}, \quad (15)$$

$$\delta \mathbf{y}_k = \mathbf{H}_k \delta \mathbf{x}_k + \mathbf{M}_k \delta \mathbf{v}_k, \quad (16)$$

where  $\mathbf{A}$  and  $\mathbf{L}$  are the process model Jacobians, and  $\mathbf{H}_k$  and  $\mathbf{M}_k$  are the measurement model Jacobians. The error definitions used to linearized are [14]

$$\delta \mathbf{x} = \begin{bmatrix} \ln(\mathbf{X} \hat{\mathbf{X}}^{-1})^\vee \\ \hat{\mathbf{x}} - \mathbf{x} \end{bmatrix}.$$

The error in the state defined on  $\mathcal{G}$  is multiplicative because  $\mathcal{G}$  is not closed under addition. Also, this is just one error definition; alternative definitions can be used as well.

The forward filter is the known MEKF [13]. The prediction step from  $\hat{\mathbf{x}}_{k-1}$  to  $\check{\mathbf{x}}_k$  is performed by integrating (12) and (13) from time  $t_{k-1}$  to time  $t_k$  assuming no process noise. The predicted covariance is given by (5) and the Kalman gain is given by (6). The state estimate correction is given by

$$\begin{bmatrix} \delta \chi_1 \\ \delta \chi_2 \end{bmatrix} = \mathbf{K}_{fk} \delta \mathbf{y}_k, \quad (17)$$

$$\hat{\mathbf{X}}_{fk} = \check{\mathbf{X}}_{fk} \exp((\delta \chi_1)^\wedge), \quad (18)$$

$$\hat{\mathbf{x}}_{fk} = \check{\mathbf{x}}_{fk} + \delta \chi_2, \quad (19)$$

where  $\delta \mathbf{y}_k = \mathbf{y}_k - \check{\mathbf{y}}_k$  and the corrected covariance is given by (8).

The backward smoothing is initialized using the state estimate and covariance output of the forward filter. The Kalman gain for the smoother is given by (9) and the smoother covariance update is given by (11). The smoother-state innovation and smoother state update are given by

$$\begin{bmatrix} \mathbf{z}_{sk}^1 \\ \mathbf{z}_{sk}^2 \end{bmatrix} = \begin{bmatrix} \ln(\hat{\mathbf{X}}_{f,k+1})^\vee \\ \hat{\mathbf{x}}_{s,k+1} - \check{\mathbf{x}}_{f,k+1} \end{bmatrix}, \quad (20)$$

$$\hat{\mathbf{X}}_{sk} = \hat{\mathbf{X}}_{fk} \exp\left(\left(\mathbf{K}_{sk} \mathbf{z}_{sk}^1\right)^\wedge\right), \quad (21)$$

$$\hat{\mathbf{x}}_{sk} = \hat{\mathbf{x}}_{fk} + \mathbf{K}_{sk} \mathbf{z}_{sk}^2. \quad (22)$$

## 5 Invariant RTS smoothing

The invariant extended Kalman filter (IEKF) [3] can be considered a variant of the extended Kalman filter (EKF), but specific to estimation problems defined on matrix Lie groups. Here, the invariant filtering framework is leveraged to introduce the invariant RTS (IRTS) smoother. Similar to traditional RTS smoothing and MRTS smoothing the forward filter in IRTS smoothing is the IEKF, and subsequently a backward smoothing step will be performed. The IEKF and proposed IRTS smoother are applicable to process models of the form

$$\dot{\mathbf{X}}(t) = \mathbf{F}(\mathbf{X}(t), \mathbf{u}(t)) + \mathbf{X}(t)\mathbf{W}(t), \quad (23)$$

where  $\mathbf{X}(t) \in \mathcal{G}$  is the state and  $\mathbf{W}(t) \in \mathfrak{g}$  is process noise where  $\mathbf{w}(t) = \mathbf{W}(t)^\vee \in \mathbb{R}^m$ . The argument  $(t)$  will once again be omitted for brevity. Given the true state  $\mathbf{X}$  and the state estimate  $\hat{\mathbf{X}}$ , the error can be defined as a left-invariant error or right-invariant error. Additionally, when the process model (excluding noise) is group affine, the error dynamics are state-independent, as stated in the next theorem.

**Theorem 1** (State-independent error dynamics [3]). If the function  $\mathbf{F}(\mathbf{X}(t), \mathbf{u}(t))$  is group affine and the error is either left- or right-invariant, then the error propagation will be state-independent.

The choice of using a left- or right-invariant error depends on the left- or right-invariant form of the measurements, as defined next.

*Definition 3 (Left- and right-invariant measurement model):* Left- and right-invariant measurements are

$$\mathbf{y}_k^L = \mathbf{X}_k \mathbf{b}_k + \mathbf{v}_k, \quad (24)$$

$$\mathbf{y}_k^R = \mathbf{X}_k^{-1} \mathbf{b}_k + \mathbf{v}_k, \quad (25)$$

respectively, where  $\mathbf{b}_k$  is some known column matrix of appropriate dimension.

When confronted with a left-invariant (right-invariant) measurement model and a group affine process model, a left-invariant error (right-invariant error) should be used [3, 4].

The error dynamics are linearized using  $\delta\mathbf{X} = \exp(\delta\xi^\wedge) \approx \mathbf{1} + \delta\xi^\wedge$ , where  $\delta\xi \in \mathbb{R}^m$  is the state of the linearized system, and the superscript for left or right has been dropped here. Because the problem considered in Section 6 has a left-invariant error, subsequent derivations assume a left-invariant error. The linearized process model is

$$\delta\dot{\xi} = \mathbf{A}\delta\xi + \mathbf{L}\delta\mathbf{w}. \quad (26)$$

The prediction step in the forward filter from  $\mathbf{X}_{k-1}$  to  $\mathbf{X}_k$  is performed by integrating the nonlinear process model from time  $t_{k-1}$  to  $t_k$ . The predicted covariance is given by (5). The left-invariant error  $\delta\mathbf{X}_{fk} = \hat{\mathbf{X}}_{fk}^{-1} \check{\mathbf{X}}_{fk}$  is the error between the predicted and the corrected state. Rearranging the error definition results in an expression for the corrected state given by

$$\begin{aligned} \hat{\mathbf{X}}_{fk} &= \check{\mathbf{X}}_{fk} \delta\mathbf{X}_{fk}^{-1}, \\ &= \check{\mathbf{X}}_{fk} \exp\left(-\left(\mathbf{K}_{fk} \mathbf{z}_{fk}\right)^\wedge\right), \end{aligned}$$

where  $\mathbf{z}_{fk} = \tilde{\mathbf{X}}_{fk}^{-1}(\mathbf{y}_k - \check{\mathbf{y}}_k)$  is the innovation, the Kalman gain is given by (6), and  $\check{\mathbf{y}}_k = \tilde{\mathbf{X}}_{fk}\mathbf{b}_k$ . To find an expression for  $\mathbf{H}_k$  and  $\mathbf{M}_k$  it is necessary to linearize the innovation. To do this, substitute (24) into the innovation expression and use the definition of the error, which results in

$$\begin{aligned}\mathbf{z}_{fk} &= \tilde{\mathbf{X}}_{fk}^{-1}(\mathbf{X}_k\mathbf{b}_k + \mathbf{v}_k - \tilde{\mathbf{X}}_{fk}\mathbf{b}_k) \\ &= \delta\tilde{\mathbf{X}}^{-1}\mathbf{b}_k + \tilde{\mathbf{X}}^{-1}\mathbf{v}_k - \mathbf{b}_k.\end{aligned}\quad (27)$$

Letting  $\delta\tilde{\mathbf{X}}_{fk}^{-1} \approx \mathbf{1} - \delta\check{\boldsymbol{\xi}}_{fk}^\wedge$  and substituting this into (27) gives

$$\begin{aligned}\mathbf{z}_{fk} &= -\delta\check{\boldsymbol{\xi}}_{fk}^\wedge\mathbf{b}_k + \tilde{\mathbf{X}}_{fk}^{-1}\delta\mathbf{v}_k \\ &= \mathbf{H}_k\delta\check{\boldsymbol{\xi}}_{fk} + \mathbf{M}_k\delta\mathbf{v}_k.\end{aligned}$$

After the forward-filter pass, the backward smoothing is initialized with the corrected state estimate  $\hat{\mathbf{X}}_{fN}$  and covariance  $\hat{\mathbf{P}}_{fN}$ . The Kalman gain used in the backward smoothing is given by (9) and the covariance update is given by (11). To find an expression describing the smoothed state estimate, first the error between  $\hat{\mathbf{X}}_{s,k+1}$  and  $\check{\mathbf{X}}_{f,k+1}$  must be defined. In the traditional RTS smoother there is the  $\hat{\mathbf{x}}_{s,k+1} - \check{\mathbf{x}}_{f,k+1}$  term which can be seen as a  $\delta\mathbf{x}$  term or as a smoother innovation term. The equivalent error in the present context, when the state is an element of  $\mathcal{G}$  and a left-invariant error is employed, is

$$\delta\mathbf{X}_{sk} = \hat{\mathbf{X}}_{s,k+1}^{-1}\check{\mathbf{X}}_{f,k+1}.\quad (28)$$

The linear representation of this error will be referred to as  $\delta\boldsymbol{\xi}_{sk}$  where  $\exp(\delta\boldsymbol{\xi}_{sk}^\wedge) = \delta\mathbf{X}_{sk}$ . Note that if a right-invariant error is used, then (28) should also be a right-invariant error. Using the linear representation of the error, an expression for the smoother-state innovation  $\mathbf{z}_{sk}$  is

$$\mathbf{z}_{sk} = \delta\boldsymbol{\xi}_{sk} = \ln\left(\hat{\mathbf{X}}_{s,k+1}^{-1}\check{\mathbf{X}}_{f,k+1}\right)^\vee.\quad (29)$$

Given that the smoother-state innovation has been defined, an expression for the smoother state estimate update can now be found. The smoother update step within a matrix Lie group context is then

$$\hat{\mathbf{X}}_{sk} = \hat{\mathbf{X}}_{fk} \exp\left(-(\mathbf{K}_{sk}\mathbf{z}_{sk})^\wedge\right).\quad (30)$$

Mind that the expressions given for the innovation and state estimate correction in the forward filter and backward smoother are derived for the left-invariant measurement model (24) using a left-invariant error definition. If however a right-invariant measurement model is used, then a right-invariant error definition must be used. This will result in

$$\mathbf{z}_{sk} = \ln\left(\check{\mathbf{X}}_{f,k+1}\hat{\mathbf{X}}_{s,k+1}^{-1}\right)^\vee,\quad (31)$$

$$\hat{\mathbf{X}}_{sk} = \exp\left(-(\mathbf{K}_k\mathbf{z}_{sk})^\wedge\right)\hat{\mathbf{X}}_{fk},\quad (32)$$

for the smoother-state innovation and smoother state estimate update, respectively.

## 6 Sample problem in $SE_2(3)$

Consider the problem of a body free to translate and rotate in 3D space. The body is equipped with a rate gyro and an accelerometer. Let  $\mathcal{F}_a$  be an inertial frame and  $\mathcal{F}_b$  a frame that rotates with the body. Point  $w$  is a fixed reference point and point  $z$  moves with the body. The states of interest are  $\mathbf{r}_a^{zw}$ ,  $\mathbf{v}_a^{zw/a}$  and  $\mathbf{C}_{ab}$ . The state can be represented as an element of  $SE_2(3)$ , that being

$$\mathbf{T} = \begin{bmatrix} \mathbf{C}_{ab} & \mathbf{v}_a^{zw/a} & \mathbf{r}_a^{zw} \\ \mathbf{0} & 1 & 0 \\ \mathbf{0} & 0 & 1 \end{bmatrix}.\quad (33)$$

Details pertaining to the matrix Lie group  $SE_2(3)$  are presented in the Appendix. The rate gyro measures

$$\mathbf{u}_b^1 = \boldsymbol{\omega}_b^{ba} - \mathbf{w}_b^1,$$

where  $\mathbf{w}_{b_k}^1 \sim \mathcal{N}(\mathbf{0}, \mathbf{Q}_k^1)$  when discretized. The accelerometer measures

$$\mathbf{u}_b^2 = \mathbf{f}_b - \mathbf{w}_b^2,$$

where  $\mathbf{f}_b$  is the specific force resolved in the body frame and  $\mathbf{w}_{b_k}^2 \sim \mathcal{N}(\mathbf{0}, \mathbf{Q}_k^2)$  when discretized. The kinematics are

$$\begin{aligned} \dot{\mathbf{C}}_{ab} &= \mathbf{C}_{ab} \boldsymbol{\omega}_b^{ba \times}, \\ \dot{\mathbf{v}}_a^{zw/a} &= \mathbf{f}_a + \mathbf{g}_a = \mathbf{C}_{ab} \mathbf{f}_b + \mathbf{g}_a, \\ \dot{\mathbf{r}}_a^{zw} &= \mathbf{v}_a^{zw/a}, \end{aligned}$$

where  $(\cdot)^\times : \mathbb{R}^3 \rightarrow \mathfrak{so}(3)$  is the linear operator that maps a three dimensional column matrix to the matrix Lie algebra  $\mathfrak{so}(3)$ . The continuous-time process model is then given by

$$\dot{\mathbf{C}}_{ab} = \mathbf{C}_{ab} (\mathbf{u}_b^1 + \mathbf{w}_b^1)^\times, \quad (34)$$

$$\dot{\mathbf{v}}_a^{zw/a} = \mathbf{C}_{ab} (\mathbf{u}_b^2 + \mathbf{w}_b^2) + \mathbf{g}_a, \quad (35)$$

$$\dot{\mathbf{r}}_a^{zw} = \mathbf{v}_a^{zw/a}, \quad (36)$$

This can be written as a function of the state matrix  $\mathbf{T}$  as

$$\dot{\mathbf{T}} = \underbrace{\begin{bmatrix} \mathbf{C}_{ab} \mathbf{u}_b^1 \times & \mathbf{C}_{ab} \mathbf{u}_b^2 + \mathbf{g}_a & \mathbf{v}_a^{zw/a} \\ \mathbf{0} & \mathbf{0} & \mathbf{0} \\ \mathbf{0} & \mathbf{0} & \mathbf{0} \end{bmatrix}}_{\mathbf{F}(\mathbf{T}, \mathbf{u}_b)} + \mathbf{T} \underbrace{\begin{bmatrix} \mathbf{w}_b^1 \times & \mathbf{w}_b^2 & \mathbf{0} \\ \mathbf{0} & \mathbf{0} & \mathbf{0} \\ \mathbf{0} & \mathbf{0} & \mathbf{0} \end{bmatrix}}_{\mathbf{W}_b}, \quad (37)$$

where  $\mathbf{W}_b = \mathbf{w}_b^\wedge$ ,  $\mathbf{w}_b = [\mathbf{w}_b^1 \mathbf{w}_b^2 \mathbf{0}^\top]^\top$  and  $\mathbf{u}_b = [\mathbf{u}_b^1 \mathbf{u}_b^2 \mathbf{0}^\top]^\top$ . The function  $\mathbf{F}(\mathbf{T}, \mathbf{u}_b)$  is group affine. In this problem a position measurement, such as a global positioning system (GPS) or ultra-wide bandwidth (UWB) measurement, provides

$$\mathbf{y}_{a_k} = \mathbf{r}_{a_k}^{zkw} + \mathbf{v}_{a_k}. \quad (38)$$

This can also be expressed as a function of the state  $\mathbf{T}_k$ ,

$$\mathbf{y}_{a_k} = \mathbf{T}_k \begin{bmatrix} \mathbf{0} \\ \mathbf{1} \end{bmatrix} + \begin{bmatrix} \mathbf{v}_{a_k} \\ \mathbf{0} \end{bmatrix}. \quad (39)$$

## 6.1 Error propagation

The measurement model in (39) is left invariant as it has the form of (24). As such, a left-invariant error  $\delta \mathbf{T} = \mathbf{T}^{-1} \hat{\mathbf{T}}$  will be used. The error propagation is

$$\delta \dot{\mathbf{T}} = \dot{\mathbf{T}}^{-1} \hat{\mathbf{T}} + \mathbf{T}^{-1} \dot{\hat{\mathbf{T}}}. \quad (40)$$

Substituting (37) into (40) and rearranging results in

$$\delta \dot{\mathbf{T}} = \mathbf{F}(\delta \mathbf{T}, \mathbf{u}_b) - \mathbf{F}(\mathbf{1}, \mathbf{u}_b) \delta \mathbf{T} - \mathbf{W} \delta \mathbf{T}. \quad (41)$$

Equation (41) is then linearized using  $\delta \mathbf{T} \approx \mathbf{1} + \delta \boldsymbol{\xi}^\wedge$  and  $\mathbf{W} = \delta \mathbf{W}$ , where  $\delta \boldsymbol{\xi} = \begin{bmatrix} \delta \boldsymbol{\xi}^\phi \top & \delta \boldsymbol{\xi}^v \top & \delta \boldsymbol{\xi}^r \top \end{bmatrix}^\top$ , resulting in

$$\delta \dot{\boldsymbol{\xi}} = \mathbf{A} \delta \boldsymbol{\xi} + \mathbf{L} \delta \mathbf{w}, \quad (42)$$

where

$$\mathbf{A} = \begin{bmatrix} -\mathbf{u}_b^1 \times & \mathbf{0} & \mathbf{0} \\ -\mathbf{u}_b^2 \times & -\mathbf{u}_b^1 \times & \mathbf{0} \\ \mathbf{0} & \mathbf{1} & -\mathbf{u}_b^1 \times \end{bmatrix}, \quad \mathbf{L} = -\mathbf{1}, \quad (43)$$

are the process model Jacobians.

## 6.2 Linearization of the measurement model

The measurement model is given by (39), and substituting this into the innovation then gives

$$\begin{aligned}
\mathbf{z}_k &= \check{\mathbf{T}}_k^{-1} (\mathbf{y}_{a_k} - \check{\mathbf{y}}_{a_k}) \\
&= \check{\mathbf{T}}_k^{-1} \left( \mathbf{T}_k \begin{bmatrix} \mathbf{0} \\ 1 \end{bmatrix} + \begin{bmatrix} \mathbf{v}_k \\ 0 \end{bmatrix} + \check{\mathbf{T}}_k \begin{bmatrix} \mathbf{0} \\ 1 \end{bmatrix} \right) \\
&= \delta \check{\mathbf{T}}_k^{-1} \begin{bmatrix} \mathbf{0} \\ 1 \end{bmatrix} + \check{\mathbf{T}}_k^{-1} \begin{bmatrix} \mathbf{v}_k \\ 0 \end{bmatrix} + \begin{bmatrix} \mathbf{0} \\ 1 \end{bmatrix}.
\end{aligned} \tag{44}$$

Linearizing (44) by letting  $\delta \check{\mathbf{T}}_k^{-1} \approx \mathbf{1} - \delta \check{\boldsymbol{\xi}}_k^\wedge$  and  $\mathbf{v}_{a_k} = \delta \mathbf{v}_{a_k}$ ,

$$\begin{aligned}
\mathbf{z}_k &\approx (\mathbf{1} - \delta \check{\boldsymbol{\xi}}_k^\wedge) \begin{bmatrix} \mathbf{0} \\ 1 \end{bmatrix} + \check{\mathbf{T}}_k^{-1} \begin{bmatrix} \delta \mathbf{v}_{a_k} \\ 0 \end{bmatrix} - \begin{bmatrix} \mathbf{0} \\ 1 \end{bmatrix} \\
&= -\delta \check{\boldsymbol{\xi}}_k^\wedge \begin{bmatrix} \mathbf{0} \\ 1 \end{bmatrix} + \check{\mathbf{T}}_k^{-1} \begin{bmatrix} \delta \mathbf{v}_{a_k} \\ 0 \end{bmatrix} \\
&= - \begin{bmatrix} \delta \check{\boldsymbol{\xi}}_k^{\phi \times} & \delta \check{\boldsymbol{\xi}}_k^v & \delta \check{\boldsymbol{\xi}}_k^r \\ \mathbf{0} & 0 & 0 \\ \mathbf{0} & 0 & 0 \end{bmatrix} \begin{bmatrix} \mathbf{0} \\ 1 \end{bmatrix} + \check{\mathbf{T}}_k^{-1} \begin{bmatrix} \delta \mathbf{v}_{a_k} \\ 0 \end{bmatrix} \\
&= \mathbf{H} \delta \check{\boldsymbol{\xi}}_k + \mathbf{M}_k \begin{bmatrix} \delta \mathbf{v}_{a_k} \\ 0 \end{bmatrix},
\end{aligned} \tag{45}$$

where

$$\mathbf{H}_k = \begin{bmatrix} \mathbf{0} & \mathbf{0} & -\mathbf{1} \\ \mathbf{0} & \mathbf{0} & \mathbf{0} \end{bmatrix}, \quad \mathbf{M}_k = \check{\mathbf{T}}_k^{-1}. \tag{46}$$

Owing to the fact that  $\mathbf{F}(\mathbf{T}, \mathbf{u}_b)$  is group affine, the measurement model in (39) is left invariant, and a left-invariant error is being used,  $\mathbf{A}$  and  $\mathbf{H}_k$  do not depend on  $\hat{\mathbf{T}}$  nor  $\check{\mathbf{T}}_k$ . The invariant framework does not guarantee  $\mathbf{L}$  and  $\mathbf{M}_k$  will not depend on  $\hat{\mathbf{T}}$  and  $\check{\mathbf{T}}_k$ , respectively, and in this specific case  $\mathbf{L}$  is constant while  $\mathbf{M}_k$  depends on  $\check{\mathbf{T}}_k$ .

## 6.3 Jacobians using MRTS smoothing

The Jacobians associated with MRTS smoothing are given by

$$\mathbf{A} = \begin{bmatrix} -\mathbf{u}_b^{1 \times} & \mathbf{0} & \mathbf{0} \\ -\hat{\mathbf{C}}_{ab} \mathbf{u}_b^{1 \times} & \mathbf{0} & \mathbf{0} \\ \mathbf{0} & \mathbf{1} & \mathbf{0} \end{bmatrix}, \quad \mathbf{L} = \begin{bmatrix} \mathbf{1} & \mathbf{0} & \mathbf{0} \\ \mathbf{0} & \hat{\mathbf{C}}_{ab} & \mathbf{0} \\ \mathbf{0} & \mathbf{0} & \mathbf{0} \end{bmatrix}, \tag{47}$$

$$\mathbf{H}_k = \begin{bmatrix} \mathbf{0} & \mathbf{0} & \mathbf{1} \\ \mathbf{0} & \mathbf{0} & \mathbf{0} \end{bmatrix}, \quad \mathbf{M}_k = \mathbf{1}. \tag{48}$$

Notice that two of the four Jacobians in (47) and (48) depend on the state estimate, while one of the four Jacobians in (43) and (46) depend on the state estimate. This may seem like a small difference, but as the results of Sections 7.1 and 7.2 show, this difference does manifest itself in the performance of the filters.

# 7 Simulations and experiments

## 7.1 Simulation parameters and results

A constant acceleration and angular velocity of  $\mathbf{a}_a^{zw/a/a} = [2.5 \ 2.5 \ 2.5]^\top 10^{-3} \text{ m/s}^2$  and  $\boldsymbol{\omega}_c^{ba} = [0.01 \ 0.01 \ 0.01]^\top \text{ rad/s}$  are used in a 300s simulation. The true initial attitude is always  $\mathbf{C}_{ab_0} =$

$\exp(\phi_0^\times)$ , where  $\phi_0 = [\frac{\pi}{4} \quad \frac{\pi}{4} \quad \frac{\pi}{4}]^\top$  rad, the initial position is  $\mathbf{r}_a^{zow} = \mathbf{0}$  m and the initial velocity is always  $\mathbf{v}_a^{zow/a} = \mathbf{0}$  m s<sup>-1</sup>. The rate gyro and accelerometer provide measurements at a rate of 100 Hz and the position measurements at a rate of 10 Hz. The rate gyro and accelerometer are assumed to have zero-mean Gaussian noise with a variance set to  $\sigma_g^2 = \frac{\pi}{36}$  rad<sup>2</sup> s<sup>-2</sup> and  $\sigma_a^2 = 5 \times 10^{-3}$  m<sup>2</sup> s<sup>-4</sup>, respectively. The noise on the position measurements is set to have a variance of  $\sigma_R^2 = 0.05$  m<sup>2</sup>. The covariance matrices for the smoother are given by

$$\mathbf{Q} = \begin{bmatrix} \sigma_g^2 \mathbf{1} & \mathbf{0} & \mathbf{0} \\ \mathbf{0} & \sigma_a^2 \mathbf{1} & \mathbf{0} \\ \mathbf{0} & \mathbf{0} & \mathbf{0} \end{bmatrix}, \quad \mathbf{R} = \sigma_R^2 \mathbf{1},$$

$$\mathbf{P}_0 = \begin{bmatrix} \sigma_{P_1}^2 \mathbf{1} & \mathbf{0} & \mathbf{1} \\ \mathbf{0} & \sigma_{P_2}^2 \mathbf{1} & \mathbf{0} \\ \mathbf{0} & \mathbf{0} & \sigma_{P_3}^3 \mathbf{1} \end{bmatrix},$$

where  $\sigma_{P_1} = \frac{\pi}{36}$  rad,  $\sigma_{P_2} = 0.05$  m s<sup>-1</sup> and  $\sigma_{P_3} = 0.05$  m. This is the standard situation, and describes the situation used to obtain the results, unless otherwise specified.

Monte Carlo simulations are performed to obtain results showing the error in the state estimator. For every Monte Carlo simulation the simulated trajectory is slightly altered from the standard trajectory. The trajectory is altered by simulating noise on the constant acceleration and angular velocity, so that the acceleration and angular velocity are slightly altered for every Monte Carlo simulation, then by integration a true value for velocity, position and attitude are obtained. The variance between every simulation of the acceleration is set to be  $\sigma_1^2 = [10^{-4} \quad 10^{-4} \quad 10^{-4}]^\top$  m<sup>2</sup> s<sup>-4</sup> and the variance of the angular velocity is set to be  $\sigma_2^2 = [10^{-5} \quad 10^{-5} \quad 10^{-5}]^\top$  rad<sup>2</sup> s<sup>-2</sup>.

Figure 1 shows the results of the mean root mean square error (RMSE) in each state for 100 Monte Carlo simulations using the IRTS and the MRTS smoothers. The lower bounds of the errorbars in Figure 1, and all forthcoming figures, are set to a percentile of 2.5 and the upper bounds of the errorbars are set to a percentile of 97.5. Although the attitude errors associated with the IRTS and MRTS smoother are about the same, the errors in position and velocity associated with the IRTS smoother are less than those associated with the MRTS smoother. The attitude errors are large

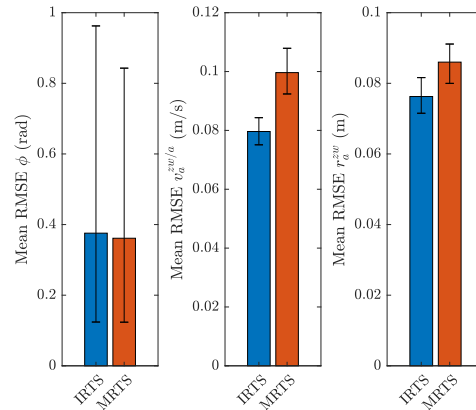


**Figure 1: The mean RMSE on the norm of the attitude (left), velocity (middle) and position (right) estimator using the IRTS and MRTS in simulation with the standard noise values.**

due to the problem set up. Specifically, the only exteroceptive measurements available are position measurements, meaning the attitude is weakly observable. The phrase “attitude is weakly observable” refers to the fact that there are no sensors that are a direct function of the attitude (e.g., such as a magnetometer), the only way to correct attitude estimates is through the position measurement, and the position measurement is not a direct function of the attitude. This is why attitude is referred to as weakly observable. Additionally, the rate-gyro measurements appear multiple times in the process model Jacobian  $\mathbf{A}$ . Therefore, rate-gyro noise impacts the accuracy of the the Jacobian  $\mathbf{A}$ , and thus

the results, especially as there is only a very weak correction in the attitude estimate via the position measurements.

Increasing the initial error of the estimator to  $\sigma_{P_1} = \frac{\pi}{6}$  rad,  $\sigma_{P_2} = 0.2 \text{ m s}^{-1}$  and  $\sigma_{P_3} = 0.2 \text{ m}$ , and thus changing the initial covariance matrix  $\mathbf{P}_0$ , gives results shown in Figure 2. It can be seen that inflating the initial error yield even more pronounced results, favoring the IRTS smoother. Specifically, the attitude errors associated with both smoother are similar, while the position and velocity errors associated with the IRTS smoother are less than those associated with the MRTS smoother.

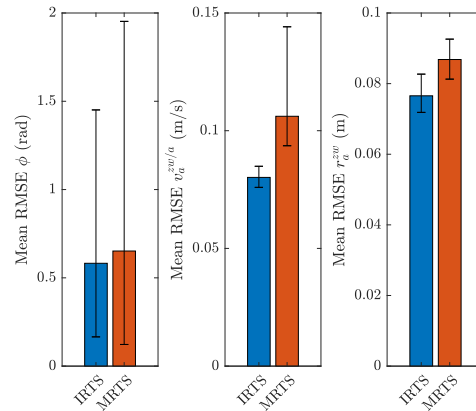


Figure 2: The mean RMSE on the norm of the attitude (left), velocity (middle) and position (right) estimator using the IRTS and MRTS in simulation using an inflated initial error.

## 7.2 Experimental results using ETH dataset

The IRTS and MRTS smoother have also been compared using data from [7]. This dataset contains the groundtruth and IMU measurements at 200Hz. The groundtruth data is used to create noisy position measurements at 10Hz as if from a GPS. The same covariance matrices  $\mathbf{P}_0$  and  $\mathbf{R}$  are used to initialize the smoother and to create the noisy position measurements. The results for 100 Monte Carlo simulations are shown in Figure 3, which describes the standard situation. The estimation errors show to be very similar for both smoothers. Just as for the simulated data, the initial error on the

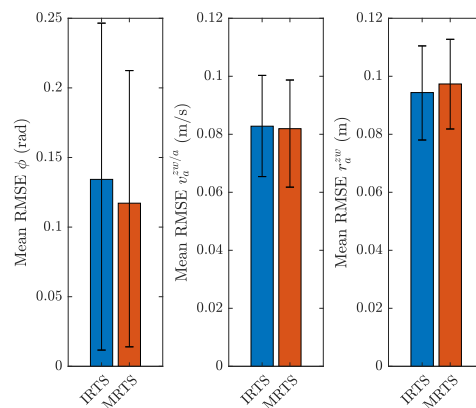


Figure 3: The mean RMSE on the norm of the attitude (left), velocity (middle) and position (right) estimator using the IRTS and MRTS on the ETH dataset.

estimator is increased to  $\sigma_{P_1} = \frac{\pi}{6}$  rad,  $\sigma_{P_2} = 0.2 \text{ m s}^{-1}$  and  $\sigma_{P_3} = 0.2 \text{ m}$ . The results of this increase in initial error are shown in Figure 4. Again, although the attitude errors as computed using the IRTS and MRTS smoothers are about the same, the position and velocity errors associated with the IRTS smoother are much lower than the errors computed using the MRTS smoother, when increasing the initial error in the state estimate.

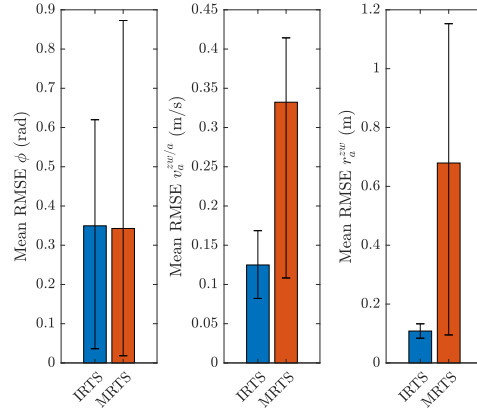


Figure 4: The mean RMSE on the norm of the attitude (left), velocity (middle) and position (right) estimator using the IRTS and MRTS on the ETH dataset for an inflated initial error.

## 8 Conclusions

The main purpose of this paper is to derive and present the IRTS smoother and benchmark it using simulated and experimental data relative to the MRTS smoother. The IRTS smoother is essentially an application of the invariant filtering of [3, 4] where left- or right-invariant error definitions, group affine process models, and left- or right-invariant measurement models are leveraged to give state-independent Jacobians. The IRTS and MRTS smoother were compared on a  $SE_2(3)$  problem using both simulated and experimental data. On the simulated data, the invariant smoother outperforms the MRTS smoother in most situations. When using experimental data both smoothers had comparable results, but for large initial errors, the invariant smoother outperforms the multiplicative smoother.

## Appendix

Three dimensional poses can be represented by the special euclidean group  $SE_2(3)$ ,

$$SE_2(3) = \left\{ \mathbf{T} = \begin{bmatrix} \mathbf{C} & \mathbf{v} & \mathbf{r} \\ \mathbf{0} & 1 & 0 \\ \mathbf{0} & 0 & 1 \end{bmatrix} \in \mathbb{R}^{5 \times 5} \mid \mathbf{C} \in SO(3), \mathbf{v}, \mathbf{r} \in \mathbb{R}^3 \right\}.$$

The matrix Lie algebra associated with  $SE_2(3)$  is

$$\mathfrak{se}_2(3) = \{ \Xi = \xi^\wedge \in \mathbb{R}^{5 \times 5} \mid \xi \in \mathbb{R}^9 \},$$

where

$$\xi^\wedge = \begin{bmatrix} \xi^\phi \\ \xi^v \\ \xi^r \end{bmatrix}^\wedge = \begin{bmatrix} \xi^{\phi^\times} & \xi^v & \xi^r \\ \mathbf{0} & 0 & 0 \\ \mathbf{0} & 0 & 0 \end{bmatrix}.$$

Additionally,  $\mathfrak{so}(3) = \{ \Omega = \omega^\times \in \mathbb{R}^{3 \times 3} \mid \omega \in \mathbb{R}^3 \}$  where

$$\omega^\times = \begin{bmatrix} 0 & -\omega_3 & \omega_2 \\ \omega_3 & 0 & -\omega_1 \\ -\omega_2 & \omega_1 & 0 \end{bmatrix}.$$

The exponential map from  $\mathfrak{se}_2(3)$  to  $SE_2(3)$  is

$$\exp(\xi^\wedge) = \begin{bmatrix} \exp_{SO(3)}(\xi^{\phi^\times}) & \mathbf{J}\xi^v & \mathbf{J}\xi^r \\ \mathbf{0} & 1 & 0 \\ \mathbf{0} & 0 & 1 \end{bmatrix},$$

where  $\exp_{SO(3)}(\boldsymbol{\xi}^{\phi^\times})$  is given by Rodrigues' rotation formula [2] and  $\mathbf{J}$  is given by

$$\mathbf{J} = \frac{\sin \phi}{\phi} \mathbf{1} + \left(1 - \frac{\sin \phi}{\phi}\right) \mathbf{a}\mathbf{a}^\top + \frac{1 - \cos \phi}{\phi} \mathbf{a}^\times,$$

where  $\phi = \|\boldsymbol{\xi}^\phi\|$  and  $\mathbf{a} = \boldsymbol{\xi}^\phi/\phi$ .

## References

- [1] E. Lefferts, L. Markley, and M. Shuster, Kalman filtering for spacecraft attitude estimation, *Journal of Guidance, Control, and Dynamics*, 5(2), 1982.
- [2] T. D. Barfoot, *State Estimation for Robotics*. Cambridge University Press, 2017.
- [3] A. Barrau and S. Bonnabel, The invariant extended Kalman filter as a stable observer, *IEEE Transactions on Automatic Control*, 62(10), 2014.
- [4] —, Invariant Kalman filtering, *Annual Review of Control, Robotics, and Autonomous Systems*, 1(1) 237–257, 2018.
- [5] G. Bourmaud, Parameter estimation on Lie groups : Application to mapping and localization from a monocular camera, *Theses, Université de Bordeaux*, Nov. 2015.
- [6] P. Chauchat, A. Barrau, and S. Bonnabel, Invariant smoothing on lie groups, 2018 IEEE/RSJ International Conference on Intelligent Robots and Systems (IROS), pp. 1703–1710, 2018.
- [7] M. Burri, J. Nikolic, P. Gohl, T. Schneider, J. Rehder, S. Omari, M. W. Achtelik, and R. Siegwart, The EuRoC micro aerial vehicle datasets, *The International Journal of Robotics Research*, 35(10) 1157–1163, 2016.
- [8] B. C. Hall, *Lie Groups, Lie Algebras, and Representations*. 2nd ed. Springer, 2014.
- [9] P. Hughes, Spacecraft attitude dynamics, *Spacecraft Attitude Dynamics and Control*, 1986.
- [10] J. A. Farrell, *Aided navigation: GPS with high rate sensors*. McGraw-Hill Education, 2008.
- [11] S. Särkkä, *Bayesian Filtering and Smoothing*. Cambridge University Press, 2013.
- [12] D. Simon, *Optimal State Estimation: Kalman, H Infinity, and Nonlinear Approaches*. New York, NY, USA: Wiley-Interscience, 2006.
- [13] M. L. Psiaki, Backward-smoothing extended Kalman filter, *Journal of Guidance, Control, and Dynamics*, 28(5) 885–894, 2005.
- [14] R. Aucoin, S. A. Chee, and J. R. Forbes, Linear- and linear-matrix-inequality-constrained state estimation for nonlinear systems, *IEEE Transactions on Aerospace and Electronic Systems*, pp. 1–1, 2019.